

NPL REPORT MAT 21

**Investigation Methods of the
 β to α Tin Allotropic
Transformation**

D Di Maio and C Hunt

NOT RESTRICTED

JULY 2008

Investigation Methods of the β to α Tin Allotropic Transformation

David Di Maio and Chris Hunt
Industry and Innovation Division

ABSTRACT

It is well known that β tin is stable only down to 13°C. Below that temperature the thermodynamic stable phase is α tin, more commonly known as tin pest. This phase has gained its fame because of the catastrophic consequences to the transforming material. This subject has become of interest because of the transition from tin-lead to lead-free in the electronics interconnection environment. Lead-free alloys contain from 95 to 99% tin and might be subjected to the β/α transformation mentioned above. In studying this phenomenon it is important to establish a way of monitoring the transformation. Past studies were mostly based on optical observations or volume change observations. However none of these methods were very precise nor do they allow continuous measurements. In this study various techniques are developed, improving the precision of the measurements and allowing for continuous observation of the transformation. Three methods were developed in this research: strain measurements, optical observation by time-lapse photography, and electrical resistance measurements. Whilst the first method could detect the inception of the transformation, it has revealed of limited applicability. The large tin volume increase (26%) associated with the transformation could not be fully detected by the strain gauges used. Better results were obtained with the optical method. In fact it was possible to generate videos allowing a better understanding of the mechanics of the transformation. The electrical resistance method has been demonstrated to be the most useful because it allows a very accurate detection of the starting point of the transformation and in measuring the transformation rate. Special “hybrid” samples were designed in order to use this technique not only with pure tin but also with tin alloys. This sample preparation has shown to shorten the incubation period. Hence this combination of sample preparation and monitoring method has proven to be a useful screening technique for verifying the propensity of tin alloys to transform.

© Crown copyright 2008
Reproduced with the permission of the Controller of HMSO
and Queen's Printer for Scotland

ISSN 1754-2979

National Physical Laboratory
Hampton Road, Teddington, Middlesex, TW11 0LW

Extracts from this report may be reproduced provided the source is acknowledged and the extract is not taken out of context.

Approved on behalf of the Managing Director, NPL,
by Dr M G Cain, Knowledge Leader, Materials Team
authorised by Director, Industry and Innovation Division

CONTENTS

1	INTRODUCTION	1
2	LITERATURE REVIEW	2
2.1	INTRODUCTION	2
2.2	MECHANISMS TO ACCELERATE GREY TIN FORMATION	2
2.3	ACCELERATORS AND DECELERATORS	3
2.4	SUMMARY	4
3	MONITORING THE TRANSFORMATION WITH STRAIN-GAUGES.....	5
3.1	INTRODUCTION	5
3.2	SAMPLE PREPARATION	5
3.3	THE STRAIN-GAUGE MEASUREMENT SYSTEM.....	6
3.4	EXPERIMENTAL SETUP.....	6
3.5	EXPERIMENTAL RESULTS	7
3.6	DISCUSSION	7
4	MONITORING THE TRANSFORMATION WITH A FOUR POINTS ELECTRICAL RESISTANCE MEASUREMENTS METHOD.....	7
4.1	INTRODUCTION	7
4.2	SAMPLE PREPARATION	8
4.3	EXPERIMENTAL PROCEDURE	9
4.4	EXPERIMENTAL RESULTS	10
4.5	DISCUSSION	15
4.6	SUMMARY	21
5	MONITORING THE TRANSFORMATION WITH A TIME-LAPSE PHOTOGRAPHY EXPERIMENT.....	23
5.1	INTRODUCTION	23
5.2	EXPERIMENTAL PROCEDURE	23
5.2.1	Equipment	23
5.2.2	Materials and Samples	24
5.2.3	Experimental Procedure.....	24
5.3	EXPERIMENTAL RESULTS	24
5.3	DISCUSSION	27
5.4	SUMMARY	31
6	CONCLUSIONS	31
7	ACKNOWLEDGMENTS	32
8	BIBLIOGRAPHY	33

1 INTRODUCTION

If pure β -Sn is kept at temperatures below 286 K for a sufficient amount of time it could potentially undergo an allotropic transformation and become α -Sn. The two phases are very different; β -Sn is a ductile metal, whilst α -Sn is a brittle semiconductor. β -Sn has a tetragonal crystal structure; α -Sn has a diamond cubic crystal structure. Most of all α -Sn has a volume approximately 26% higher than β -Sn [1]. This normally has a catastrophic effect on the transformed material, which tends to crack and fall apart due to the volume expansion. Whilst this could potentially be devastating if it happened on an electronic assembly in service, studies have shown so far that it can happen on pure tin, and in rare occasions on alloys, such as Sn-0.5Cu [2, 3] and SnZn [4]. There is a possible risk that this phenomenon could occur in current electronic assemblies since all the SnPb replacement alloys have a high tin content, such as the SAC (Sn-Ag-Cu) alloy family. For this reasons more studies are required to make sure that these alloys are really risk-free so that they can reliably be used in low-temperature applications. The transformation is normally quite slow, and could require months or even years before showing the first signs of occurrence. However, it is possible to “artificially” accelerate this phase by introducing a seed in contact with the tin. This is a material with a similar crystal structure and lattice parameter to that of α -Sn [5]. Substances that share these properties are shown in Table 2.1.

The introduction of these crystals accelerates the nucleation of the first α -Sn crystals, which will form in the neighbouring regions. The transformation then propagates radially from this area [1]. This acceleration of the incubation period is not expected to occur in the field. However, it makes it possible to study the transformation in different materials in a reasonable timescale. The inoculation process works on the principle that the crystals of the foreign substance produce a strain on the β lattice to provide an impetus to force the transformation and provide a growth point of an almost identical structure for which the α tin to grow on. As such it lowers the energy of the system, by helping it to reach its thermodynamic equilibrium. The inoculator crystal and tin need to have a favourable orientation to each other in order for the transformation to occur. Hall [6] has suggested an orientational relationship between the diamond cubic α and the tetragonal β lattices $(001)_{\beta} \parallel (001)_{\alpha}$ and $[001]_{\beta} \parallel [110]_{\alpha}$. The β crystal has to expand during the transformation process in order to accomplish this. A favourable orientation can speed up the so called “incubation period”, defined as the time before the first nucleation commences. A better contact between the seeds and tin can also increase the probability of transformation and reduce the incubation period. This can be achieved by introducing the seed into molten tin and hence removing air gaps between the two [7]. So far it has been possible to observe the transformation only by removing the sample from the freezer and hence altering its progress. This research aims to find methods for monitoring the transformation in situ. This is essential to obtain quantitative objective data and clarify the risk that commercial tin alloys could transform. Three methods are investigated in this study: monitoring the transformation by sensing the volume change, by sensing the electrical resistance change and by a time-lapse photography technique.

2 LITERATURE REVIEW

2.1 INTRODUCTION

At temperatures below 13.2 C, the thermodynamically stable form of tin is the body centred cubic grey tin (α -tin) rather than the more common tetragonal white tin (β -tin). Grey tin is a brittle semiconductor and has a volume 26% higher than white tin [8]. Due to this volume change eventually tin decomposes into powder, hence the name “tin pest”.

Many different studies have been carried out in order to determine the mechanism of this allotropic transformation. A recent paper by Styrkas [7] summarises them well. A similar classification is used here, together with the references to other studies that mentioned the same processes. In the same paper Styrkas observes that no transformation is possible without an inoculator, which can be any substance with a similar crystal structure and lattice parameter to that of α -tin.

Whilst inoculators are necessary to induce the transformation, other elements and factors can speed up the process, but alone are not enough to produce it. These will be referred here as accelerators as opposed to factors that can slow down the process (decelerators).

2.2 MECHANISMS TO ACCELERATE GREY TIN FORMATION

1. Initiation from pressed-in seeds (molecular contact). The transition is induced by seeds with a lattice parameter and chemical bonding close to α -Sn, which are embedded in β -Sn to ensure molecular scale contact. The seed materials found in literature are shown in Table 2.1. It is generally noted that not all authors refer to pressed-in seeds, and in most cases, the contact condition is not specified (see mechanism 2). Pressed-in seeds are necessary to insure molecular scale contact [7].

Table 2.1: Inoculators that induce the β -Sn to α -Sn transformation.

Substance	System	Lattice Parameter
α -Sn	Cubic, (diamond)	a = 6.489
Si	Cubic, (diamond)	a = 5.43
Eutectic Sn/Zn	Cubic	
Ge	CCP	a = 5.65
InSb	Cubic, (diamond)	a = 6.489
CdTe	Cubic, (diamond)	a = 6.41
Metastable Ice	Cubic, (diamond)	a = 6.36
Hg	Rhombohedral	a = 3.005
SnO	Tetragonal	a = 3.80, c = 4.84

2. Initiation with a seed without molecular contact. Infection of a seed in contact with the surface of tin is only possible in the presence of atmospheric water vapour, whose condensation on a seed leads to the formation of cubic ice [7]. In this case, elements like InSb and CdTe (see Table 2.1) act as incubators for the formation of an epitaxial layer of cubic ice. Cubic ice has a similar lattice parameter to α -tin (Table 2.1)

and it is presumed that this ice, transfers the lattice structure of the seed to the tin surface by penetrating into micropores of tin oxide film (SnO). This explains also why infection occurs in cases when the seed is not strictly in contact with the tin sample. Seeding is ensured by the formation of a layer of epitaxial cubic ice, which eventually gets in contact with tin [7]. The distance between the seed and the tin influences the incubation time, defined as the time before nucleation starts. There is enough experimental evidence to show that cubic ice can act as a seed for the transformation without the direct presence of a pre-introduced inoculator; this can happen only when the atmosphere contains water vapour and microparticles of substances similar in structure to α -Sn [7].

3. Initiation from inert substances. Experimental evidence has shown that β -Sn placed in a tube that previously contained α -Sn can transform. The transformation occurs in this case because the inert substance (e.g. glass) was in contact with the seed, which in turn lead to an epitaxial layer of metastable ice. After the seed is removed, the cubic ice remains on the glass and can act as a seed for the transformation [7, 9]. Styrkas claims that when the seed is removed, the metastable water re-mains on the glass even at room temperature as “structured water” and that if β -Sn is placed on the glass and then cooled, it transforms into α -Sn. In that paper it is not mentioned however, if the glass surface was checked for the presence of some residuals of the original seeds.

4. Initiation from SnO. The oxide that normally forms on β -Sn is SnO₂. On the surface of α -Sn, SnO forms instead. If this transformed tin is then brought to room temperature, SnO is partially retained. This oxide can act as a seed for a further re-transformation, in case the tin is cooled again (memory effect) [7]. The reason for this is not clear, its structure is fairly close to the required diamond cell, but the lattice parameter is not similar to that of α -Sn (see Table 2.1).

5. Initiation from water immersion. Sn samples brought in contact with a seed immersed in water may also undergo the transition. Styrkas [7, 9] observes that the mechanism is not completely explained but it may be similar to mechanism 2 and under the effect of seeds, adjacent water takes on the required structure [7, 9, 10, 11]. Another explanation is that indium antimonide, if present in water, influences the electrochemical potential of the system. Its presence also, could create an oxidation process, which would raise the acidity of the solution and partly transform the SnO₂ on the tin surface into SnO, whose structure is suitable for inducing the transformation [9].

2.3 ACCELERATORS AND DECELERATORS

It was observed that the transformation is not immediate but requires an incubation [12], defined as the time before the transformation commences. This stage of the transformation is followed by nucleation and growth of the new phase. A clear distinction is made between the mechanisms of α -Sn formation, described in the previous section, and the accelerator factors, defined here as (i) factors that shorten the incubation period and (ii) factors that increase the growth rate.

Much research has been carried out in order to determine the factors that produce an accelerated incubation time and increased growth rate. They are reported in Table 2.2 and referred simply to “accelerators” and “decelerators”. No distinction is made between the factors that produce and accelerated incubation time and those that increase the growth rate because this distinction was found in literature only in few cases. For example, the

growth rate after nucleation was found to be independent of mechanical treatment and surface conditions, but dependent on temperature [1]. Various authors do not agree with the temperature at which the transformation is the fastest, this was found to be in the range -20 to -50 °C. The rate of transformation was also found to decrease when the specimen is cemented to a substrate, especially when the film is very thin [1].

Table 2.2: Factors that accelerate and decelerate the incubation time and growth rate.

Accelerators	Decelerators
Chemical treatments to remove the SnO ₂ film on tin surface [7]	Surface Oxidation
Contact with some chemicals like an ethanol solution of pink salt [1, 8]	Surface treatments with water ethanol glycerol and other substances capable of binding (solvating) structured water, fully eliminates the possibility of the transition [7].
Presence of impurities As, Co, Mg, Mn, Si, Te, Zn [1] Al [1, 4, 8] Ga, Ge [1, 4] Ge Cu [4, 5] Au, Fe, In, Ni, P [4]	Presence of impurities: Sb [11, 4, 12, 16] Pb [1] Bi [1, 4, 5, 12, 14, 16] Ag [1, 4, 17] Cd [1, 15] Al [112] Au [1] In [17]
Cold Working, bending, twisting [1, 12, 14]	Annealing
Stressing the tin in tension [12]	High Pressure (90 atm) [1]
Larger grain size [8, 12, 14]	Finer grains [1, 12, 14]
Electroplated tin [1, 12]	Hot dipped tin [12]
	Slow growth of the initial white Sn crystal [1]
	Storage of Sn in vacuum, ethanol, acetone or a dessicator causes no transition, since water vapour necessary for structuring is missing in such system [9].
Temperature in the range -20 to -50 °C [1, 5, 8]	
Thin films of Sn cemented to a substrate [1]	
Reactor irradiation [1, 15]	

2.4 SUMMARY

From this literature research, it can be concluded that the allotropic transformation from β -tin to α -tin can only occur in presence of an inoculator. This must have a similar crystal structure and lattice parameter to that of α -tin. In this context the role of cubic ice appears to often play a pivotal role, although this has been difficult to establish unequivocally. More research would be required to clarify the role of water and to establish if atmospheric water could induce the transformation when in the right condition.

There is good agreement among the authors about the factors promoting a rapid transformation. However there are some discrepancies on the effect of Sb, Al and Au (see Table 2.2). Also, Sweatman [8] found that Fe was the element that most increased the transformation process, whilst Becker [1] found only little effect from it, together with Ni

and Cu. It would be important to carry out further research in this direction and clarify what elements hinder the process and what elements promote it and under what temperature range. This could help in understanding if lead-free alloys (and in case which) could potentially be at risk from tin pest.

3 MONITORING THE TRANSFORMATION WITH STRAIN-GAUGES

3.1 INTRODUCTION

Probably the most noticeable feature of the β/α transformation is the 26% increase in volume that is probably unique amongst solid-to-solid transformations. It appears logical to exploit this feature of the transformation to monitor its progression. This has been done in the past using dilatometry. In this case samples were immersed in silicone oil and the progress of the transformation was monitored via the height of the liquid [2]. This immersed condition, however, does not reflect the condition faced by solder joints on a printed circuit board (PCB). For this reason the volume change was measured here using a strain gauge system.

3.2 SAMPLE PREPARATION

For this test a high purity (4N)¹ tin sample was used. The sample was created by melting a small amount of tin in an oxidised steel mould, with a shape of a cylinder. These cylindrical samples were 40mm long and 4mm wide. One extremity of the Sn sample was then temporarily melted with a torch and 5 mg of CdTe powder were pushed inside the metal using some tweezers. This was done to make sure there was “molecular” contact between the seed and the Sn (see Section 2.2).

¹ Purity of tin is often indicated as 2N, 3N or 4N, meaning that is 99%, 99.9% or 99.99% pure respectively.

3.3 THE STRAIN-GAUGE MEASUREMENT SYSTEM

The volume change on the tin sample was measured using a temperature compensated Wheatstone Bridge. This is shown in Figure 3.1. Resistors R1 and R3 have the same electrical resistance, and the strain gauges are the same. If no force is applied to the sample, the bridge is in a perfectly balanced condition and the voltmeter shows 0 volts. Both gauges are attached to the same test specimen. One is placed where the measurements need to be taken, whilst the other gauge is isolated from all mechanical stress, and works only as a temperature compensation device. If the temperature changes, the resistance of both gauges will change by the same percentage, and the bridge's state of balance will remain unaffected. Only a differential resistance (difference of resistance between the two strain gauges) produced by a strain on the test specimen can alter the balance of the bridge.

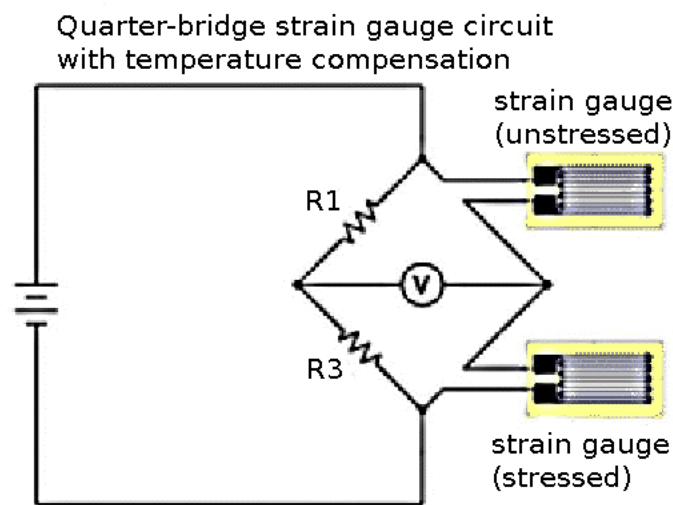


Figure 3.1: Temperature Compensated Wheatstone Bridge.

3.4 EXPERIMENTAL SETUP

The active strain gauge of the system described above was attached to the surface of the tin sample. This was then placed in a freezer, at a constant temperature of -35 C. The resistance on the Wheatstone bridge was measured with a Pico logger² connected to a PC.

² <http://www.picotech.com>

3.5 EXPERIMENTAL RESULTS

Once the voltage change of the bridge was recorded, this was converted into a strain. The curves obtained with this process are shown in Figure 3.2.

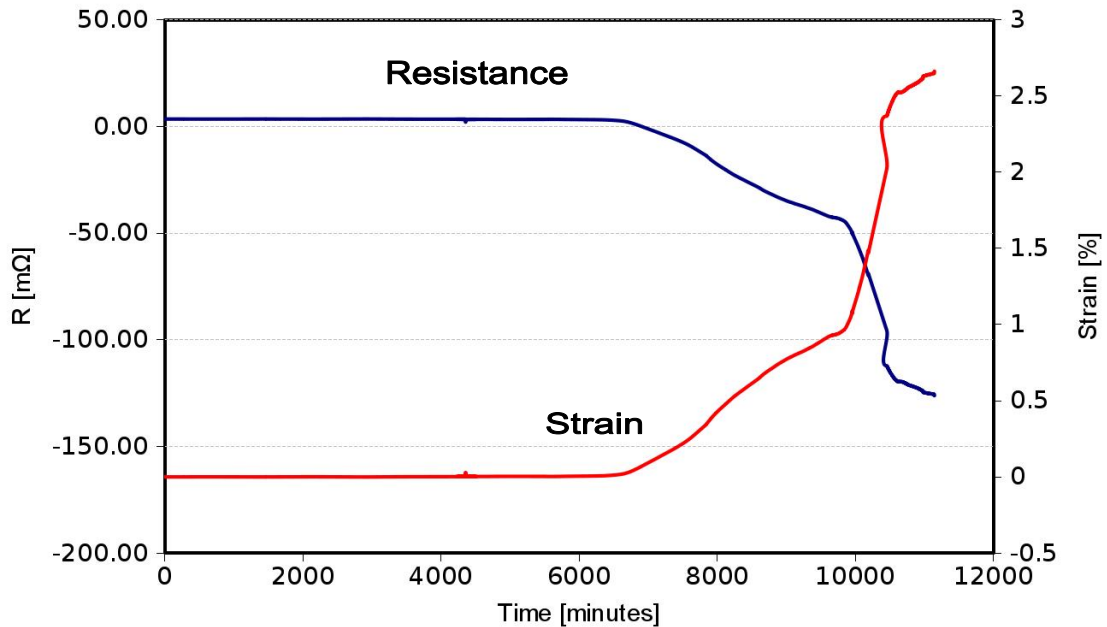


Figure 3.2: Graph showing the resistance change in the Wheatstone Bridge and the corresponding strain in the sample.

3.6 DISCUSSION

This monitoring method demonstrated to show well the onset of the transformation. As can be seen from Figure 3.2, the strain started increasing after 6000 minutes (100 h). However the maximum recorded value is just 2.7%, which is a small amount of the maximum 26% expected for the full transformation. This is due to the fact that the strain gauge that was used had around 2.7% of maximum allowed transformation. This limits the usability of this method, which is good for detecting an initial change but it is not for monitoring the whole transformation. Theoretically strain gauges that allow larger strains could be used, however it was not possible to find one on the market that would cover the full strain range of this transformation.

4 MONITORING THE TRANSFORMATION WITH A FOUR PROBE ELECTRICAL RESISTANCE METHOD

4.1 INTRODUCTION

The first monitoring method described in Section 2 was based on the volume expansion property of the transformation. A second monitoring method was investigated. In this case the property that was used is the change in a physical property of the material. As it

was observed in Section 1, β -Sn is a metal, whilst α -Sn is a semiconductor. Hence the conductivity of α -Sn is lower than that of β -Sn. Furthermore, this material property is temperature dependent and the dependency has an opposite behaviour for the two phases. In metals, like β -Sn, the conductivity decreases with increasing temperature because of higher scattering. In semiconductors, like α -Sn, conductivity increases with increasing temperature because more electrons will jump from the valence to the conduction band. As the transformation experiments are performed at a relatively low temperature (-35°C) the difference between the two conductivities will be even higher. This property is exploited in the measuring method developed here. This consists of a four probe electrical resistance measurement of an inoculated sample kept at -35°C .

4.2 SAMPLE PREPARATION

The samples that were used for this study could be defined as hybrid samples. One gram of Sn was melted with a torch and 5 ± 0.5 mg of CdTe powder were pushed inside the metal. The sample was solidified in an oxidised steel mould in the shape of a small cylinder, with the inoculated part at one extremity. The second part of this sample consisted of 1 g of Sn alloy, for example Sn-Cu. The two parts were then placed next to each other in the mould and the torch was used to melt selectively on the surfaces separating the two parts. Tweezers were used to push slightly the samples while they were melted and remove any interface between them. The torch was then kept for 5 seconds on the interface to allow the diffusion of the alloying element into the pure tin. This generated a gradient in composition between the pure Sn and the alloy. Sn-Cu, Sn-Ag, Sn-Zn, Sn-Ni, Sn-Bi, Sn-In, Sn-Pb and Sn-SAC305 hybrid samples were prepared for this study (see Table 4.4). These are referred here as “simple hybrids”. Another type of sample was prepared for this research; this will be called here a “triple hybrid”. The sample preparation is the same as for the simple hybrid, but in this case two pieces of Sn alloy are required. They are placed on each side of the pure tin part. In this case, the inoculation is performed at the centre of the tin sample. At the end of the process there should be two gradients in composition between the central part (Sn) and the extremities (Sn-alloy). The same alloys used for simple hybrids were used also for triple hybrids (see Table 2). The sample geometry is sketched in Figure 4.1.

Table 4.1: Composition of the simple and triple hybrids of various Sn alloys (determined by inductively coupled plasma).

Materials	% Second element in Triple hybrid (%)	% Second element in Triple hybrid
Sn - Ag	5.75	0.35
Sn - Cu	1.76	0.46
Sn - Ni	0.39	0.39
Sn - Zn	2.78	0.38
Sn - Bi	19.00	0.49
Sn - In	3.65	0.43
Sn - Pb	17.2	0.49

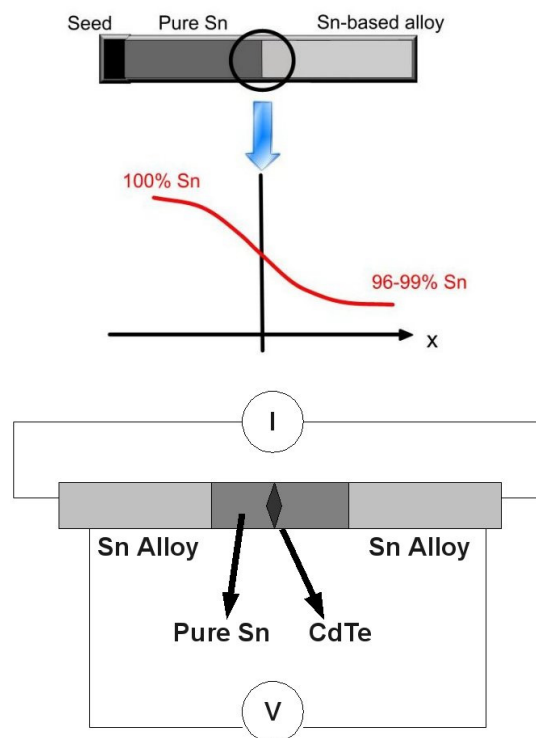


Figure 4.1: Sample geometry: simple and triple hybrids.

4.3 EXPERIMENTAL PROCEDURE

With the triple hybrid samples, constant monitoring of the transformation through a 4-point electrical resistance measurement is possible. This measurement technique is based on the fact that the resistivity of α -Sn at -35°C is roughly one order of magnitude larger than that of β -Sn. In α -Sn, which is a semiconductor, the resistivity is higher at lower temperatures whilst in β -Sn (metal) the situation is the opposite. This measurement

technique was first explored on pure tin. Two wires were attached on each side of the sample. This was achieved by locally melting the sample with the torch and then inserting the wire. One pair of wires were connected to a power supply, the other pair were connected to a voltage logging system. The sample was powered with a current of 1 A. The logging device was connected to a computer recording the electrical resistance of the sample every minute. A real-time graph of the resistance change was also produced. Using this technique on a simple hybrid sample would not be possible as the sample is not symmetric. For the triple hybrid the wires were connected to the sample's extremities. These are the last to transform and hence the electrical connection was lost only at the end of the transformation. The triple hybrids of the alloys shown in Figure 1 were prepared and electrically connected to the 4-point measurement system. Then, they were placed in a freezer, at the constant temperature of -35 °C. The power was applied and the logging system was started.

4.4 EXPERIMENTAL RESULTS

The plot of the electrical resistance change with time is shown in Figure 4.2. The plot is shown in a log-log scale so that small initial changes in electrical resistance could be observed on the same graph. It can be seen that the incubation period is different for the various materials and so is the slope of the curves. With this method, it is possible to detect the early stages of the transformation. When the first changes in the electrical resistance were observed on the logging system, no clear optical signs were detected from simple observations. For example, the samples with the lowest slope (SnPb and SnBi) still seemed untransformed when the last optical observation was made, but the electrical resistance had increased indicating the start of the phase transformation. Simple hybrid samples were used only for qualitative observations, and EDX analyses were performed on partially transformed samples. These are shown in Figures 4.3 to 4.10 together with SEM images of the same samples.

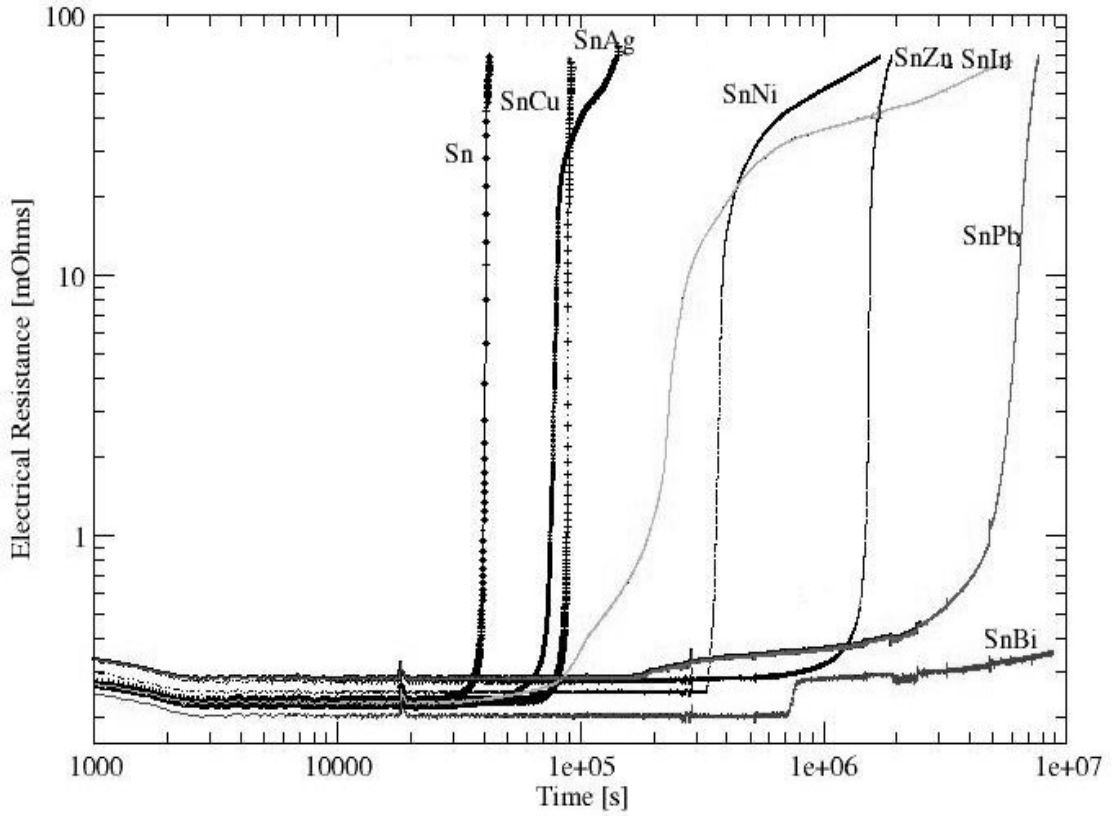


Figure 4.2: Electrical resistance change of Sn alloys during the transformation at -35 °C.

Sn-Ag

Element	Weight%	Atomic%
Ag L	7.11	7.76
Sn L	92.89	92.24
Totals	100.00	

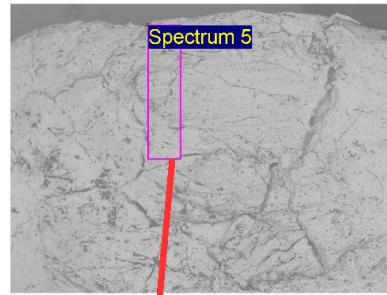
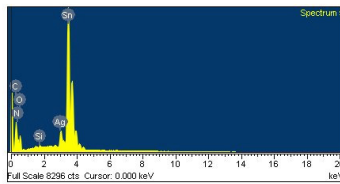


Figure 4.3: EDX of SnAg sample.

Sn-Cu

Element	Weight%	Atomic%
Cu K	4.06	7.32
Sn L	95.94	92.68
Totals	100.00	

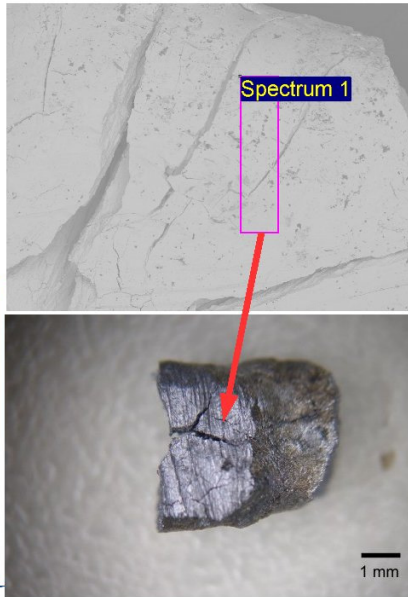
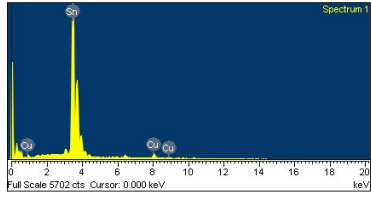


Figure 4.4: EDX of SnCu sample.

Sn-Zn

Element	Weight%	Atomic%
Zn K	2.72	4.84
Sn L	97.28	95.16
Totals	100.00	

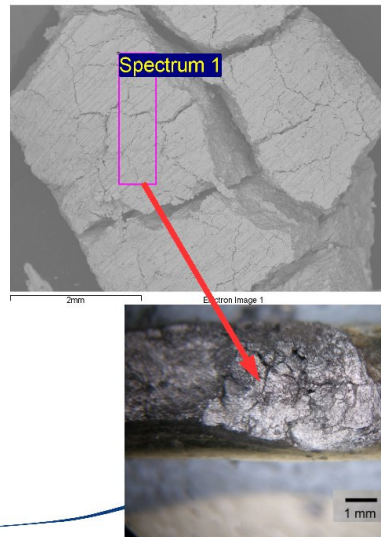
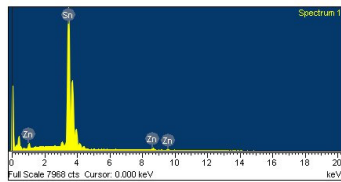


Figure 4.5: EDX of SnZn sample.

Sn-Ni

Element	Weight%	Atomic%
Ni K	1.77	3.51
Sn L	98.23	96.49
Totals	100.00	

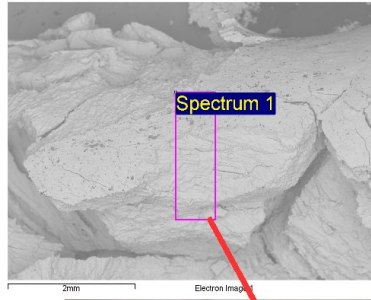
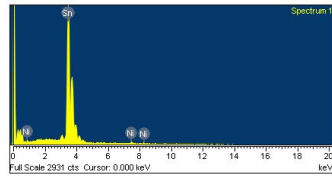


Figure 4.6: EDX of SnNi sample.

Sn-In

Element	Weight%	Atomic%
In L	1.27	1.31
Sn L	98.73	98.69
Totals	100.00	

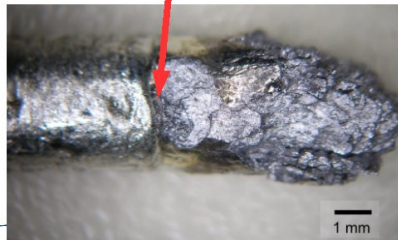
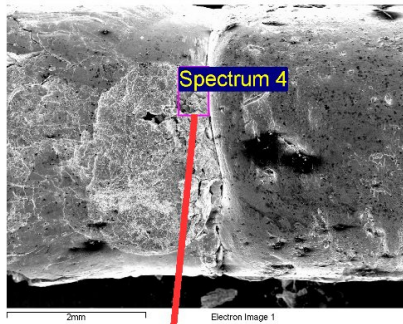
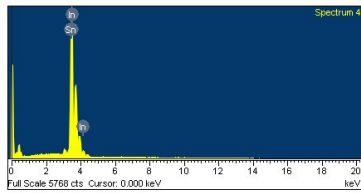


Figure 4.7: EDX of SnIn sample.

Sn-Bi

Element	Weight%	Atomic%
Sn L	98.97	99.41
Bi M	1.03	0.59
Totals	100.00	

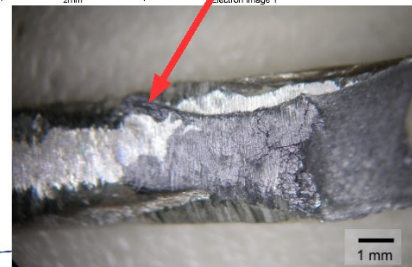
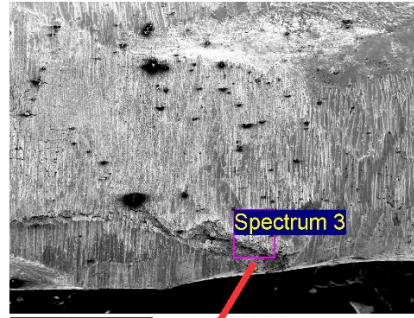
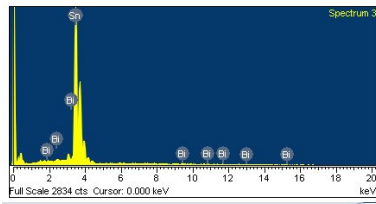


Figure 4.8: EDX of SnBi sample.

SnPb

Element	Weight%	Atomic%
Sn L	98.38	99.07
Pb M	1.62	0.93
Totals	100.00	

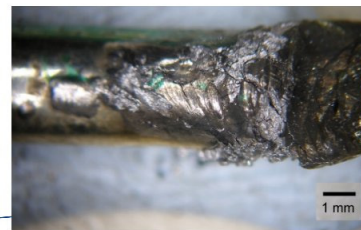
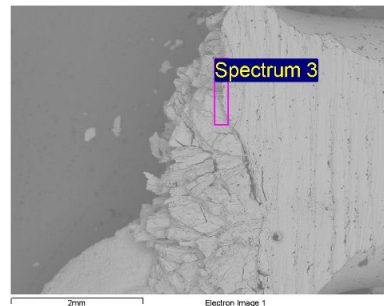
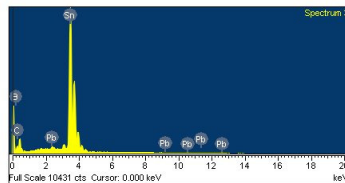


Figure 4.9: EDX of SnPb sample.

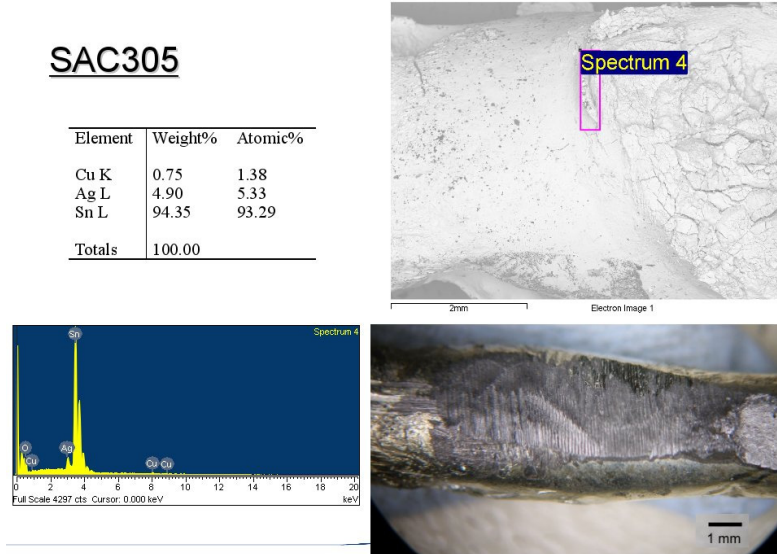


Figure 4.10: EDX of the SAC305 sample.

4.5 DISCUSSION

As the geometry of the sample and the resistivities of α and β tin are known, it is possible to calculate the theoretical electrical resistance. Samples had the following geometry:

$$\begin{aligned}
 r_0 &= 1.8 \cdot 10^{-3} \text{ m (radius)} \\
 l_0 &= 40 \cdot 10^{-3} \text{ m (length)} \\
 \rho_\beta &= 1.1 \cdot 10^{-7} \text{ } \Omega\text{m (resistivity of } \beta \text{ tin at } 0 \text{ }^\circ\text{C)} \\
 \rho_\alpha &= 4 \cdot 10^{-4} \text{ } \Omega\text{m (resistivity of } \alpha \text{ tin at } 0 \text{ }^\circ\text{C)} \\
 \text{from which } S_0 &= 10.3 \cdot 10^{-6} \text{ m}^2 \text{ (cross sectional area)} \\
 \text{and } V_0 &\approx 411 \cdot 10^{-9} \text{ m}^3 \text{ (sample volume)}
 \end{aligned}$$

Hence the theoretical electrical resistance of the untransformed β tin sample is $R_\beta = \rho_\beta l_0 / S_0 = 0.43 \text{ m}\Omega$, where S_0 is the cross sectional area of the sample.

Taking into account the 26% volume increase of α tin, the theoretical R_α is $1.4 \text{ } \Omega$. The experimental values of R_β is practically the same as the theoretical value. Differences are due to small geometrical changes between the samples and because the calculation above was done at $0 \text{ }^\circ\text{C}$, temperature at which the resistivity values for α and β tin could be found in literature.

The maximum measured value of R_α was $70 \text{ m}\Omega$, which is 2 orders of magnitude lower than what theoretically expected. This is consistent with not all the β Sn transforming into α Sn. The fact that the electrical resistance is much lower than the expected value can be explained taking into account how the transformation proceeds in the sample. The

transformation first propagates on the surface and then progressively into the bulk, as discussed in the next section.

A simple model can be used to verify how the electrical resistance changes during the transformation. This concentric cylinders model assumes that:

- The sample is initially a bar of β Sn;
- The transformation occurs equally on all the surface at the same time and the slowly proceeds inwards;
- The inner diameter of the β Sn shrinks linearly with time;
- The incubation period is neglected;

A schematic drawing of the sample geometry is shown in Figure 4.11.

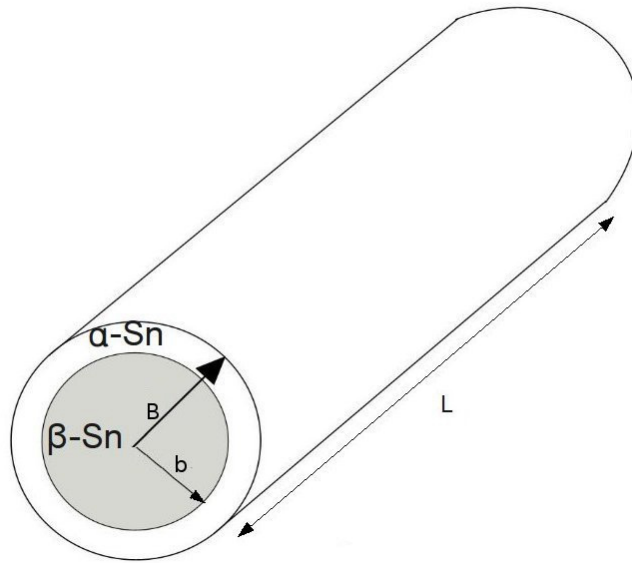


Figure 4.11: Geometry of the concentric cylinder model. This assumes that the sample is a bar and that the surface transforms first to form the first cylinder, all at the same time.

Using this simplified model, the total resistance can be seen as the resistance of alpha tin and the resistance of beta tin in parallel. The resulting resistance is then:

$$R_{tot} = \frac{R_{\alpha} R_{\beta}}{R_{\alpha} + R_{\beta}} \quad (1)$$

$$R_{tot} = \frac{\rho_{\alpha} \rho_{\beta} L}{\pi [b^2 (\rho_{\alpha} - \rho_{\beta}) + \rho_{\beta} B^2]}$$

Where R_{α} and R_{β} are separate resistances of α and β tin, ρ_{α} and ρ_{β} are the two resistivities, L is the sample length, b and B are the radii as shown in Figure 4.11. Figure 4.12 shows how the total electrical resistance changes as a function of t , using this

model. The experimental result for pure tin is superimposed. From Figure 4.12 it can be observed that:

- The model does not predict well the first part of the transformation. This is due to the simplification that all the surface transforms at the same time

The model works better by the end of the transformation. For resistance values well below the theoretical fully transformed α -Sn resistance, the material transformed is almost 100% (see Figure 4.12). This is in accordance with the optical observation of the sample, which appears to be completely transformed.

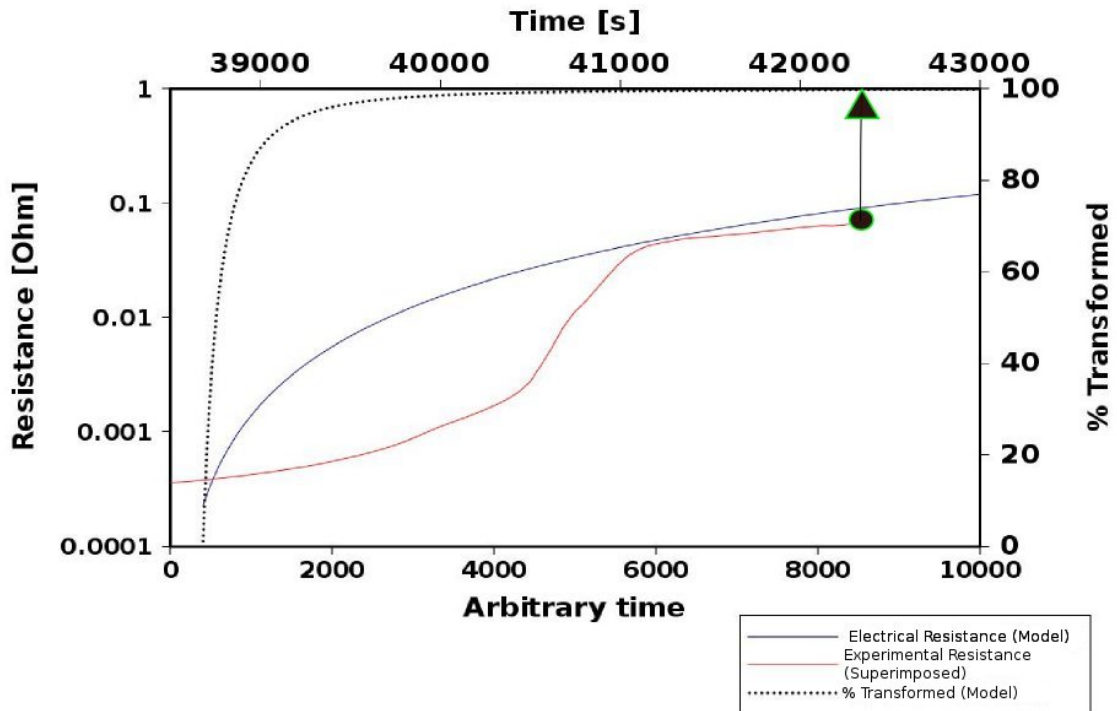


Figure 4.12. Change of resistance according to the model, superimposed experimental results for pure Sn and % transformed material.

In reality the total resistance is probably a mixture of resistances in series and in parallel, as some of the core material in the sample will transform too, however it's accurate enough in explaining why the sample does not show a higher resistance at the end of the transformation. The much lower resistance of the untransformed material dominates over the resistance of the α tin. It is quite likely that some of the Sn was untransformed at the core of the sample when the experiment was terminated.

The experimental curve, obtained from the real-time monitoring method, is first flat, during the incubation time, but the slope changes as soon as the transformation begins. Other studies [14, 18] found similar curves using dilatometry. The dilatometry technique involves immersing samples in a liquid and hence this method does not reflect the conditions that a real solder joint would be facing in the field.

Previous studies have shown that the tin pest transformation complies with the Avrami's equation [18]:

$$1 - f(t) = \exp(-At^k) \quad (2)$$

where $f(t)$ is the fraction of material transformed, t is the time and A and k are experimental constants. In this study however this relation could be verified for pure tin only. The other samples present compositional gradients that make the transformation rate change across the length.

The shape of the tin transformation curve was also confirmed by a second model. This consisted in a 3D computer simulation and was performed in the following way:

- The crystal structure was assumed to be a 3D square lattice. A lattice size of 20x10x10 cells was used for the calculation. In Figure 4.13 a simplified 2D grid is shown.
- One of the squares is taken as the inoculation point (top left square is used in Figure 4.13).
- The crystals surrounding the inoculation point are subject to transformation in the next stage.
- The next stage produces a random transformation in one of these neighbours.
- At each stage each transformed cell can originate a new transformation. The process is repeated till the whole sample is transformed.
- The % of material transformed is measured at each stage.
- The electrical resistance of each cell is in series with cells of the same row and in parallel with cells of different rows.

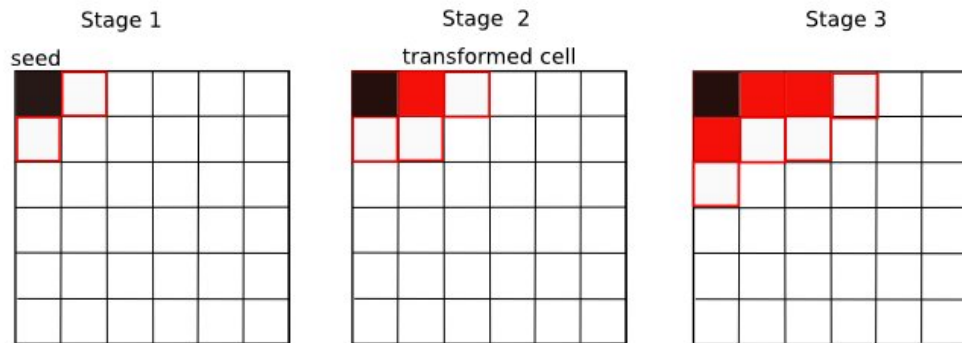


Figure 4.13: Simulation of tin pest transformation.

The result of the simulation is shown in Figure 4.14. The experimental result for pure Sn is superimposed. It can be observed that:

- The transformation volume follows a curve in accordance to equation (1).
- The first part of the transformation is well simulated by the model (up to 40% transformed).
- The model steps up in resistance reaching the theoretical R_α whilst the experimental results show a much lower value. In this model it is assumed that the transformation can occur in every direction with the same probability. In reality it was observed that the material transforms on the external surfaces first and then progresses in the bulk. This later part of the transformation was better simulated by the concentric cylinder model described before. This also indicates that the parts of the curve with a gentle slope refers to a transformation occurring parallel to the surface, whilst increased slope indicates a transformation perpendicular to the surface.

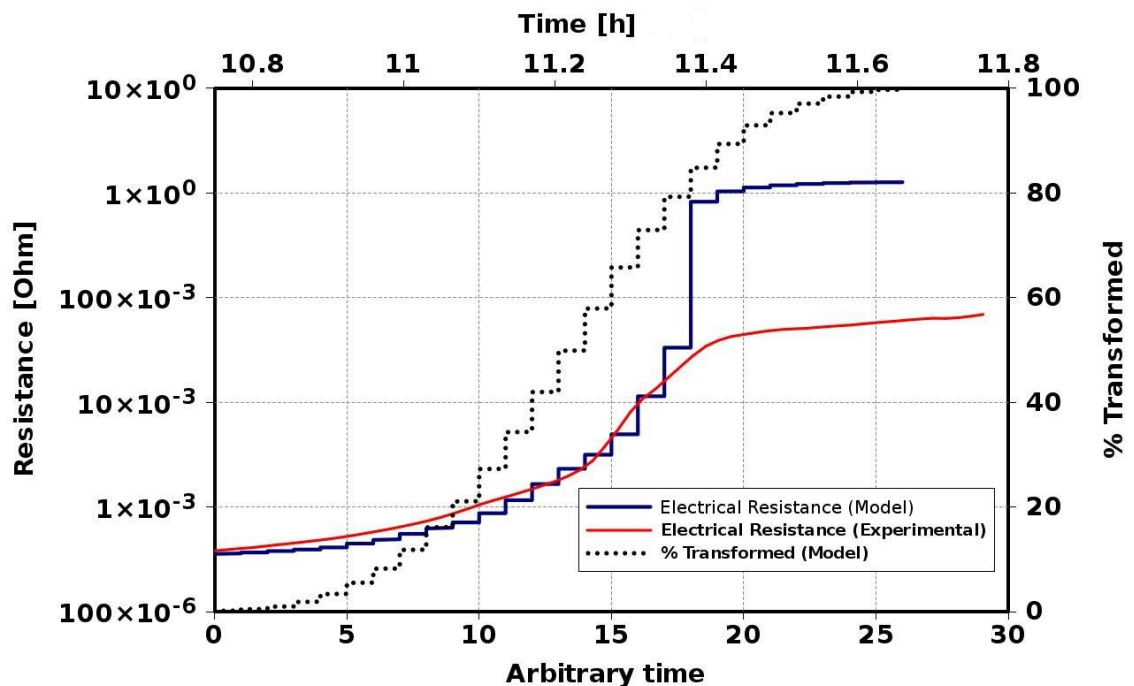


Figure 4.14. Electrical resistance of pure Sn during the transformation: experimental data and computer simulation curves.

Ideally it should be possible to determine the amount of transformed material at each point in time from the curves of Figure 4.2. However neither of the two models predicts accurately the full course of the transformation. For this reason it is not possible to directly correlate the amount of material transformed with the measured electrical resistance over the full transformation. The initial stages of the transformation of the 3D model fit reasonably well with the initial observed increase in resistance. The resistance measured during the final stages of the experimental observations follow the concentric cylinders model described before.

In order to compare the various alloys the following procedure was used:

- 1) The initial point of the transformation was arbitrarily chosen as the point at which the ratio $T_i = \frac{R_{t_i} - R_0}{R_0}$ was equal to 0.15, where R_{t_i} is the resistance at time t_i and R_0 the initial resistance value.
- 2) The time needed to reach this point was taken as the incubation time.
- 3) The point at which the ratio $T_t = \frac{R_{t_t} - R_0}{R_0}$ was equal to 4 was used as a reference point to compare the alloys. R_{t_t} is the resistance value at this time t_t . This corresponds to a 400% resistance increase compared to the initial value. For the samples used here R_{t_t} was equal to approximately to 1 mΩ.
- 4) The time difference $\Delta t = t_i - t_t$ was recorded.

A graphical description of this procedure is shown in Figure 4.15.

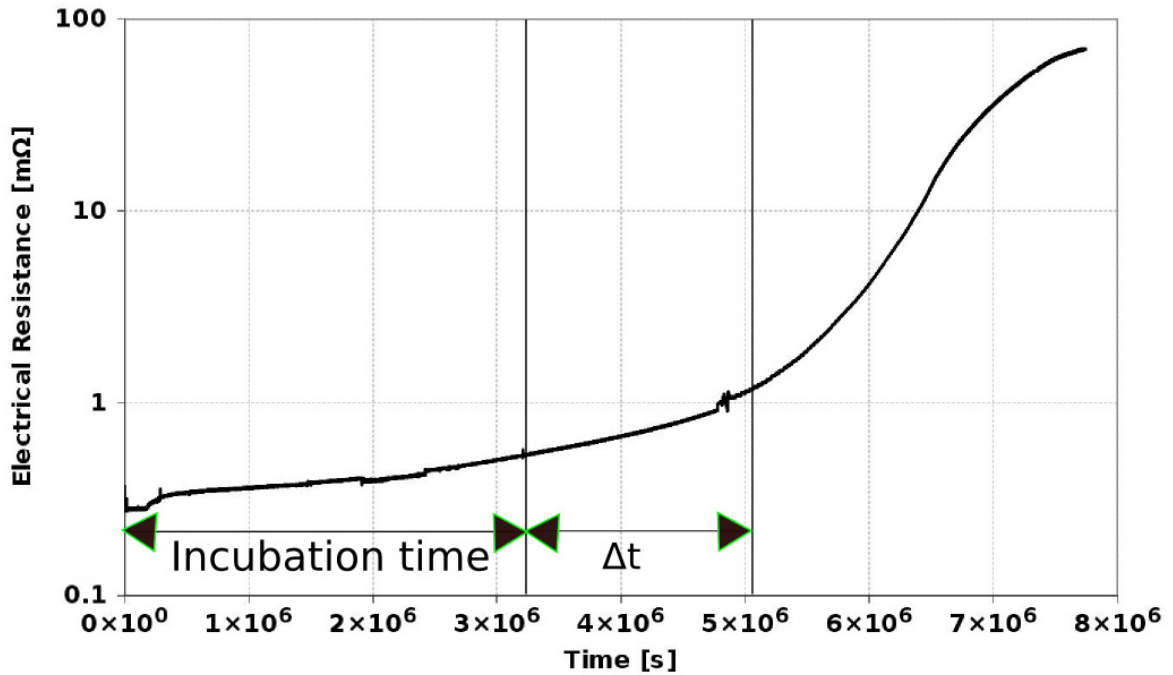


Figure 4.15: Electrical resistance change during the transformation of Sn- 0.4Pb. The incubation time and the Δt required to reach T_t are shown.

The non-dimensional quantity “propensity of transformation” is defined here as:

$$P = \frac{t_{0,Sn} + \Delta t_{Sn}}{t_{0,X} + \Delta t_X} \quad (3)$$

where $t_{0,Sn}$ and $t_{0,X}$ are the incubation times for pure tin and the alloy X and Δt_{Sn} and Δt_X are the time differences described above for pure tin for the alloy X. These numbers can be used to scale various alloys in terms of risk of transformation. From Table 4.5 it is

possible to see that the propensity of transformation of 0.4% SnPb and a SnBi alloys is respectively 3 and 4 order of magnitudes less than that of pure Sn. The Sn-Bi alloy had not reached the point at which the ratio of point (3) above could be calculated, so the slope was used to estimate Δt and the propensity to transformation.

Table 4.2: Incubation time, Δt and propensity to transformation for various alloys. (* estimated from the final slope)

	Incubation time t_i [h]	Δt [h]	Propensity to transformation
Sn	9.8	1.5	1
SnAg	15.3	5.7	$5.3 \cdot 10^{-1}$
SnCu	21.7	2.8	$4.6 \cdot 10^{-1}$
SnIn	19.3	35.7	$2.0 \cdot 10^{-1}$
SnNi	93.4	7.3	$1.1 \cdot 10^{-1}$
SnZn	271.8	146.5	$2.7 \cdot 10^{-2}$
SnPb	78.3	1375.1	$7.8 \cdot 10^{-3}$
SnBi	205.2	$22 \cdot 10^3$ (*)	$5.1 \cdot 10^{-4}$ (*)

A great variation in the incubation time between the various alloys was also observed. This time does not seem to be related to the transformation rate or more precisely to the rate of resistance change. For example the SnPb sample starts transforming earlier than SnNi, but the latter reached the maximum $70 \text{ m}\Omega$ when the SnPb resistance was only $0.4 \text{ m}\Omega$, indicating that SnPb was still at an early stage of the transformation. It is interesting to observe that the propensity to transformation is lower for the 3 alloys that are soluble in tin, which are Zn, Pb and Bi. Also their incubation time is highest. Amongst the alloys that are not soluble only Ni shows a relatively long incubation.

The incubation time is required for the first nucleation sites to form, which means that a few atomic layers will have to rearrange in the cubic crystal structure. To do this, they require some space around them. For this reason free surfaces tend to transform first (see next section). This also explains why in cold worked samples the incubation time is considerably shorter [2] and why alloys with soluble elements have longer incubation times (the pure tin regions in these alloys are smaller).

It would be very difficult to establish the exact moment when the first atomic layers have transformed, as there is not any practical method for measuring this change. The physical properties like volume (described in the previous section) or the electrical resistance will need a minimum amount of transformed material before the change can be physically observed. It is possible that the long time during which nothing seems to happen is in partly due to the long time required for the first signs of the transformation to be observable.

4.6 SUMMARY

The triple hybrid method for preparing samples was found very effective in accelerating the transformation which otherwise would take too long to observe. The monitoring

method with the 4 probes was useful for scaling the propensity of various alloys to the tin pest transformation. This study was focused on binary alloys however commercial alloys are also being studied and will be the topic of future publications.

This study has confirmed previous qualitative observations that indicated Bi and Pb as the main elements for preventing the transformation of tin. In particular it was found that additions of Bi has a propensity of transformation 4 orders of magnitudes smaller than that for pure Sn. It was estimated that in order for this alloy to reach the point T_t (chosen here as a comparison point) it would take 2.5 years. However a longer monitoring time would be required to confirm this. In fact there are three possible scenarios to what could happen: 1) the rate stays the same and the estimation is right (surface transformation dominates as the slope would stay the same); 2) the transformation penetrates into the bulk, and hence increasing the resistance value at higher rates; 3) the transformation stops when Bi rich areas are encountered.

In conclusion this experimental set up revealed to be successful in obtaining the transformation in a relatively short time for both pure tin and alloys, by significantly reducing the incubation time. This procedure can then be used for testing the propensity of transformation of the current and future commercial Sn alloys.

5 MONITORING THE TRANSFORMATION WITH A TIME-LAPSE PHOTOGRAPHY EXPERIMENT

5.1 INTRODUCTION

A third method investigated here for monitoring the tin transformation, is an optical method. This does not allow precise quantitative measurements of transformation rates, however it was found to be very useful in characterising more generally the transformation process. In particular it has helped in understanding the mechanics of the transformation and its propagation process.

5.2 EXPERIMENTAL PROCEDURE

5.2.1 Equipment

The equipment used to produce time-lapse photography of tin pest consisted of: a vacuum chamber with a transparent top, a liquid cooling system, a microscope and an imaging system. The vacuum chamber was used in order to avoid ice formation on the tin samples. The model used for this study was produced by Island Scientific and consisted of a steel cylindrical container with a toughened glass top (see Figure 5.1). An external pump was connected to the chamber system to achieve a vacuum level of 1 bar.

In order to reach the low temperatures required for the allotropic transformation, a peltier element was used (SuperCool PE-127-20-15). This had 62 mm sides and a thickness of 4.6 mm. By setting suitable values of voltage and current, the peltier element can achieve a high level of cooling on the top side, provided that the heat produced at the bottom side can be removed promptly. For this reason, the peltier was placed on a fully enclosed aluminium tank, connected in series with a liquid cooling system. A water and glycol mixture was pumped into the aluminium tank from a reservoir where it was stored and kept at a temperature of approximately -5°C . This temperature was obtained by using a Haake DC30 chiller. A thermocouple was placed on the peltier surface in order to obtain real-time temperature measurements.

A thermistor (an NTC $2\text{ K}\Omega$ at 25°C), part of a power divider circuit, was also placed on the surface of the peltier. The electrical resistance of this component was related to the temperature value by using a calibration curve. This was calculated using the thermocouple described before. These temperature readings were transmitted to a PC using a data logger PICO ACD-11. They were stored by a Visual Basic software package and used to control the power supply connected to the peltier element in order to set the desired temperature.

A digital camera (Olympus SP-350), attached to an optical stereo microscope (Brunel Microscope IMXTZ) was used to take the time-lapse photos. The sample was illuminated by an LED ring attached to the microscope objective. The camera was controlled by the software InPhoto Capture³, which could take photos at pre-defined time intervals and transfer them directly to the computer's hard disk. The same images were also used with the imaging system LaVision Davis Strainmaster System to study the movement of the surface more accurately.

³

www.akond.net

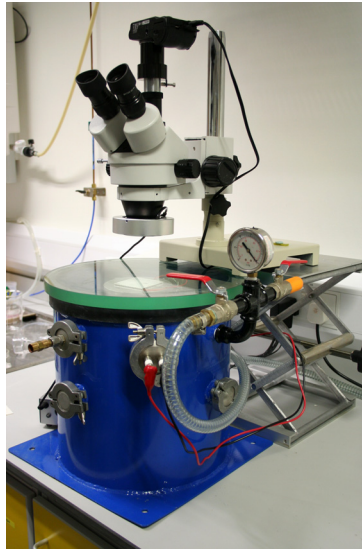


Figure 5.1: Vacuum chamber used for the time-lapse photography experiment.

5.2.2 Materials and Samples

The β -Sn/ α -Sn allotropic transformation was studied on very pure tin (99.99% Sn). As reported by Williams [5], the incubation time for this allotropic transformation can be greatly reduced by introducing in the tin a material with the same crystal structure of α -Sn. The samples were prepared by melting a small amount of tin in a mould (50 mm long, 2 mm thick and 2 mm wide). On some parts of the surface 3-5 g of Cd-Te powder were placed, and the area was brought briefly to melting temperature, to facilitate the “molecular contact” of the inoculator to the tin [7]. Afterwards the sample surface was manually polished with SiC paper until the surface was reasonably flat for optical microscopy observation.

5.2.3 Experimental Procedure

The tin samples prepared with the above procedure were placed on top of the peltier, in the vacuum chamber. Plasticine was used attach the sample to the surface. When the cooling liquid reached -5 °C the software activated the power supply controlling the peltier. The set temperature for the peltier element was -35 °C. At the same time the time-lapse photography software was started. The time interval between each photo was set to two minutes. At the end of the transformation the photos were edited by adding a scale bar and joined together to produce a motion video.

5.3 EXPERIMENTAL RESULTS

Each of the tested samples completed the transformation in less than 48 hours. Several samples were tested, in order to observe the transformation at different magnification. Two samples were inoculated in several areas on the surface; two samples were inoculated only at one extremity.

Some of the frames obtained from 3 different samples are shown in Fig 5.2 a, b and c. The arrow in the first frame depicts where the seed was placed. It can be observed that the transformation starts from the region where the inoculator was placed and then propagates in the surrounding areas. Frames 2 and 3 of Figure 5.2 c show that the expansion is radial from the starting point. The average speed at which the interface moves was measured from the sequence of images and was found to be $9\pm 1 \mu\text{m}/\text{min}$, $11\pm 1.5 \mu\text{m}/\text{min}$ and $5\pm 0.8 \mu\text{m}/\text{min}$ for the three samples shown in Figure 5.2. It was also possible to observe that the transformation rate was not constant in the whole sample, as it can be inferred from Figure 5.3.

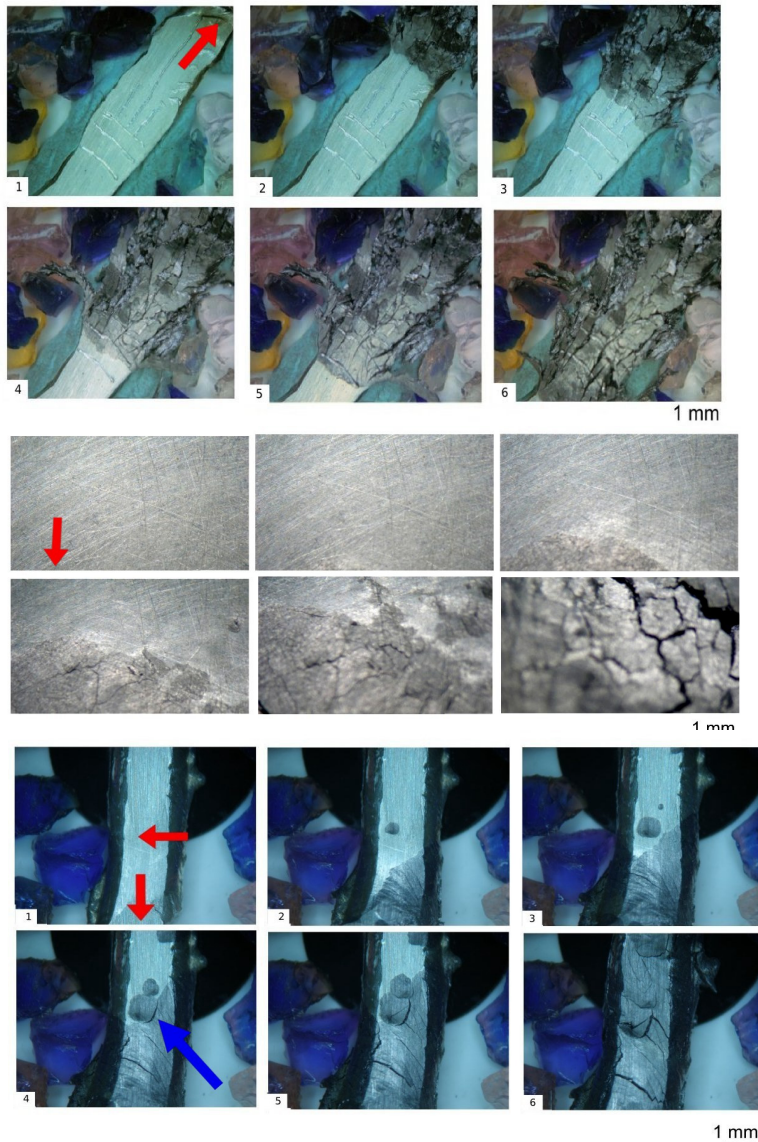


Figure 5.2: (a) Tin sample with seed on one extremity. (b) Tin sample at higher magnification. (c) Tin sample with multiple seeding.

The volume growth associated with the transformation can also be easily observed from the same images. The percent increase in area from frame 1 in Fig 5.2 c to frame 6 was

calculated to be around $18 \pm 1\%$, which is compatible with the theoretical volume increase of α -Sn of 26%. In fact if a unit cube increases uniformly its volume by 26%, its area should increase by 17%.

It was also observed that cracks form on the surface, and they tend to be perpendicular to the direction of the moving interface (or parallel to the propagation direction), as shown in Figure 5.2.

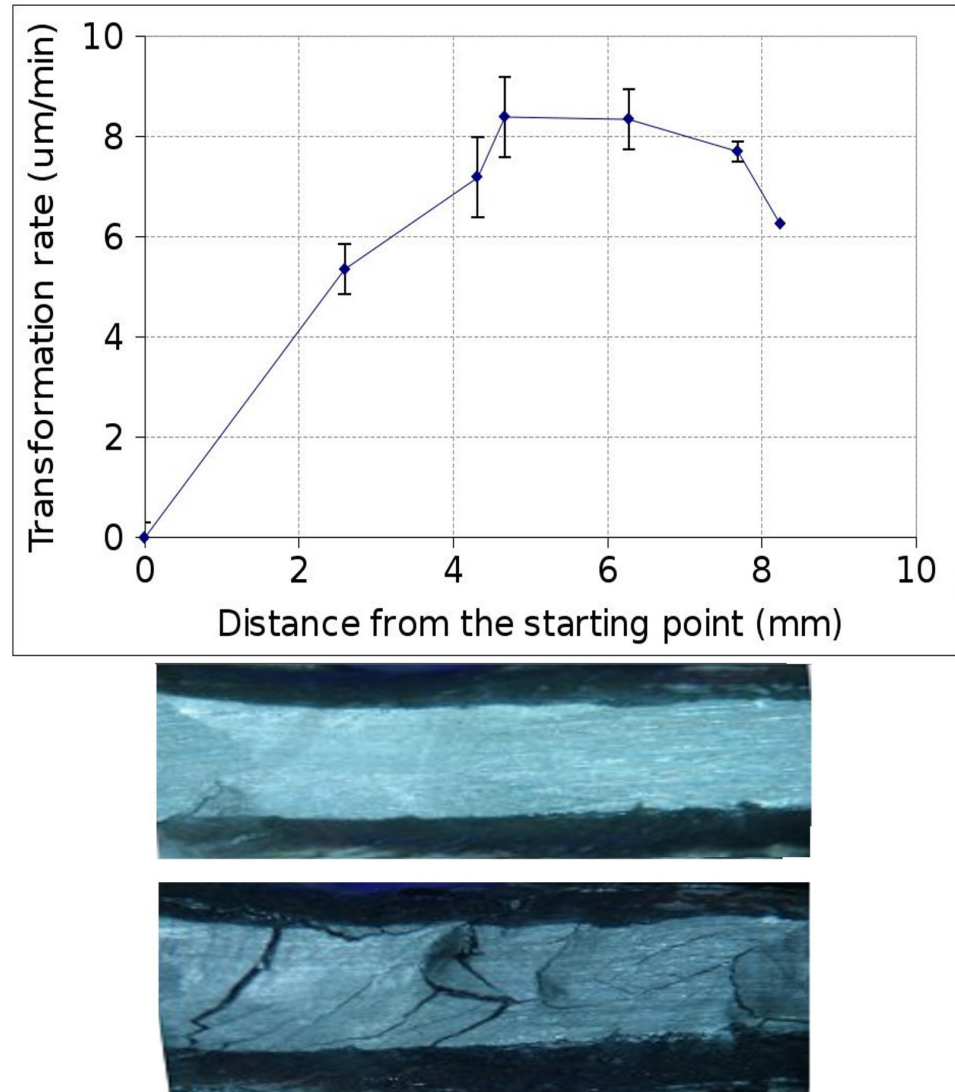


Figure 5.3: Variation of the transformation rate on the sample surface in $\mu\text{m/s}$. The corresponding sample at the beginning and at the end of the transformation is shown.

5.3 DISCUSSION

The formation of α -Sn requires an incubation time [12], defined as the time before the transformation commences. This incubation time ceases when the nucleation of the first few atomic layers of the new phase initiates. The long incubation (compared to the transformation rate) is probably due to the time required for few β -Sn atoms to “align” to the inoculator crystal. Despite this is a thermodynamically favourable (lower energy) state, the low temperature reduces the kinetics of the transformation. This incubation time is a function of the temperature in two concurrent ways. Firstly a lower temperature increases the driving force of the transformation and hence the free energy difference G increases. At the same time, the low temperature reduces the thermal energy of the lattice. This decreases the probability that atoms realign to the new structure [14]. The length of the incubation time depends on which of these two factors prevails.

Once the first energy barrier is overcome and the first α -Sn is nucleated, the transformation proceeds faster, as the neighbouring atoms have the same orientation of the tin that has already transformed. The higher magnification test showed that the propagation seems to follow scratches on the surface parallel to the propagation direction. This would confirm that the transformation starts on the surface [19] and is facilitated by defects of the crystal structure, such as those created by plastic deformation [14]. This is consistent with the fact that in the presence of a surface or a crystal defect (vacancy or dislocation), less energy is required to allow the rearrangement to the new structure. Bornemann and Rogers [14, 20] report that compressive forces tend to stop the transformation, hence if the nucleation occurred in the bulk, the compressive force of the surrounding material, created by the volume expansion, would tend to stop the transformation.

The initially transformed material on the surface creates compressive and shear stresses at the internal α/β interface, as shown in figure 5.4. The corresponding coherency strain at the α/β interface [21] will produce cracks near the interface between the two phases, parallel to the propagation direction of the transformed material. These newly created free surfaces are now available for further transformation (see figure 5.4). A similar transformation mechanism was reported also by Plumbridge [3]. The image analysis performed using the imaging system LaVision Davis Strainmaster System software show also that in the surrounding untransformed area significant strains are developed. These are due to the compression generated by the already transformed tin. The arrows in Figure 5.5 indicate this.

The peeled surfaces will tend to “roll” out of the surface, due to the expansion of the next inner layer of α tin that is still attached to the sample and has started to transform (see Figure 5.4). At the same time, the volume expansion will tend to create cracks that are parallel to the propagation direction. These types of cracks were also described in [6]. Similar images from a SEM of a partially transformed sample can be seen in Figure 5.6. Here, multiple layers of transformed material can be observed, consistently with the proposed model of propagation of the transformation.

Cracks can also appear when two isolated areas that are transforming interfere with each other. At the boundary the mismatch in the transformed α -tin will lead to a crack. This can be seen in Figure 5.12 (c) frames 3 and 4 (blue arrow). This research has established a method for observing *in situ* the allotropic transformation from β -Sn to α -Sn. A model for the macroscopic transformation of tin has been suggested, based on these observations. It is deduced that the transformation starts on the surface and gradually proceeds in the bulk by small layers of materials transforming sequentially. This creates

the disintegration of the upper layer material, which peels away. Two types of cracks are formed. One type is parallel to the propagation direction. These cracks are formed by the stress generated between transformed and untransformed regions. Another type of crack is perpendicular to the propagation direction. These are formed when two transforming regions meet.

The time-lapse photography method developed here was used to study the case of β to α transformation, but with only small changes could be used for studying the reverse transformation. Other future research fields where this method could be applied include the effect of temperature variations on the transformation rate and the study of the transformation in alloys, in particular lead-free alloys, which are of interest to the electronics industry.

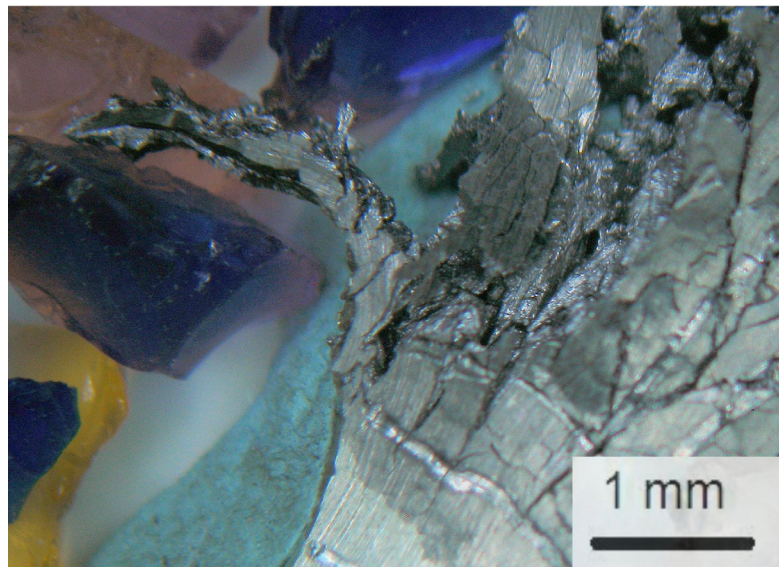
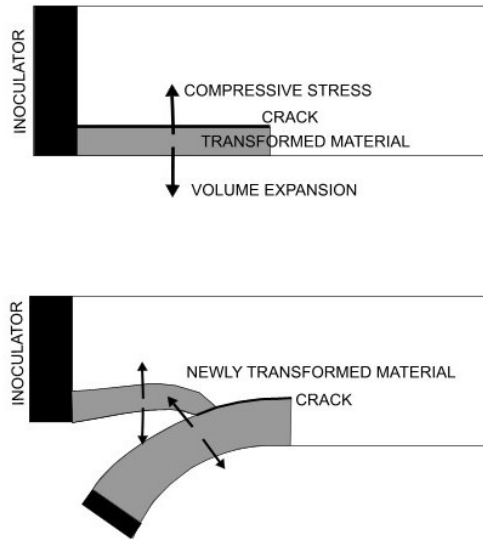


Figure 5.4: Peeling process

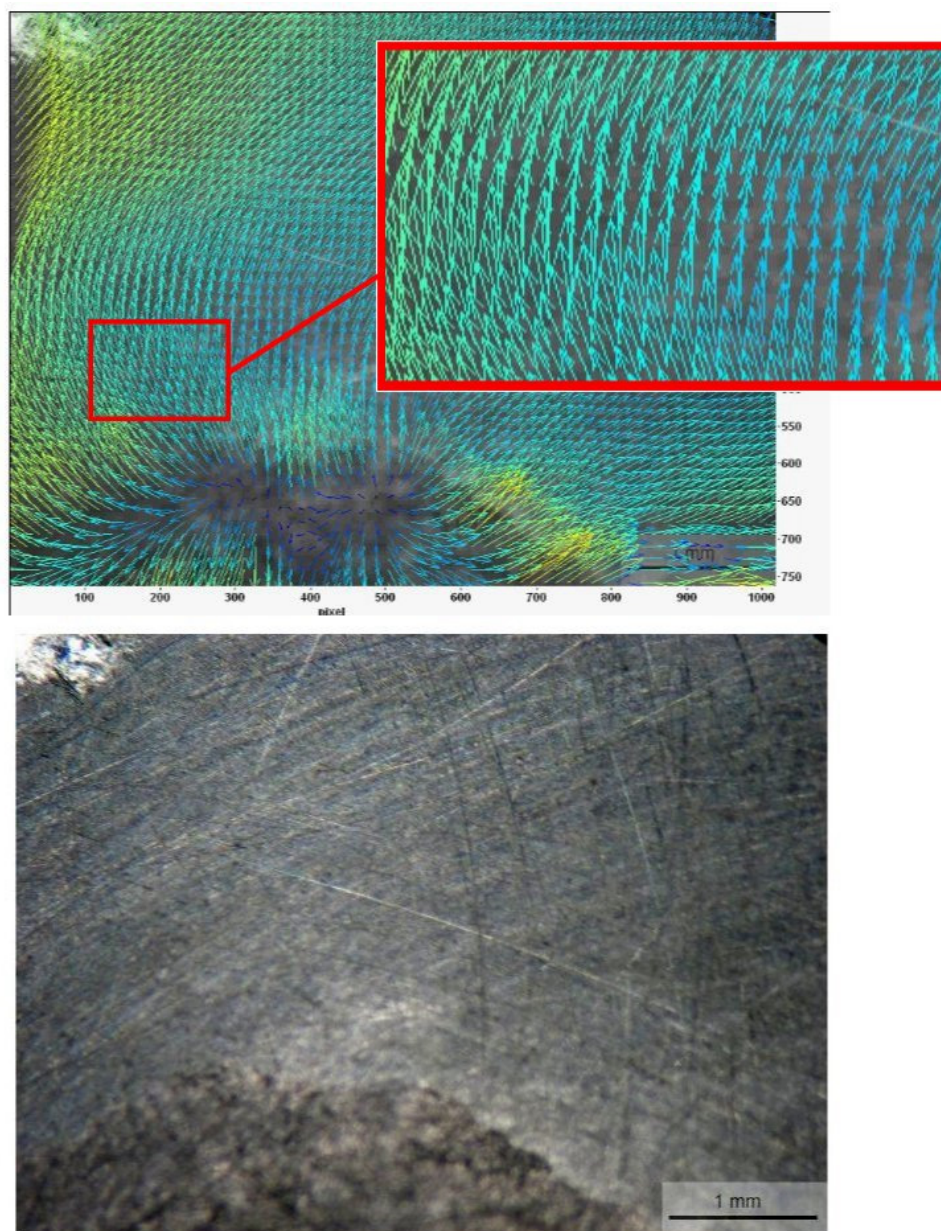


Figure 5.5: Image Analysis

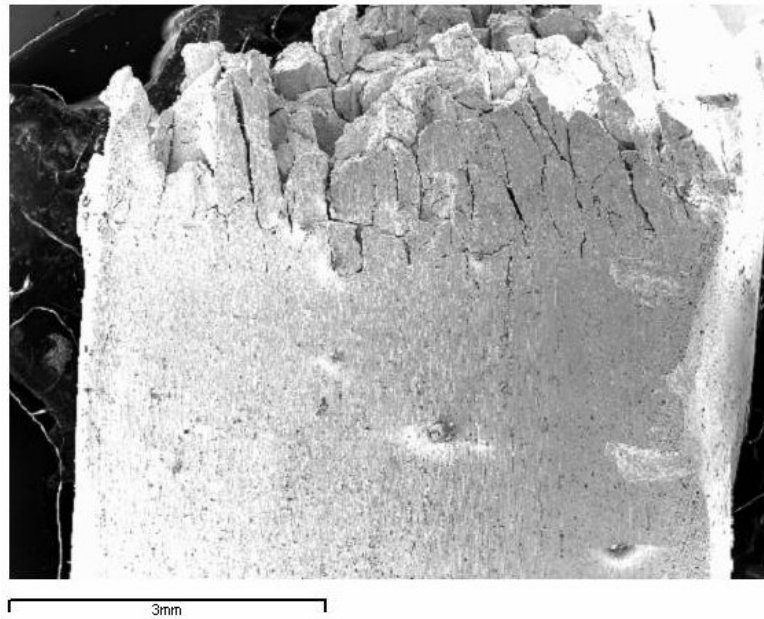


Figure 5.6: SEM Image of the peeling process

5.4 SUMMARY

This research has established a method for observing *in situ* the allotropic transformation from β -Sn to α -Sn. A model for the macroscopic transformation of tin has been suggested, based on these observations. It is deduced that the transformation starts on the surface and gradually proceeds in the bulk by small layers of materials transforming sequentially. This creates the disintegration of the upper layer material, which peels away. Two types of cracks are formed. One type is parallel to the propagation direction. These cracks are formed by the stress generated between transformed and untransformed regions. Another type of crack is perpendicular to the propagation direction. These are formed when two transforming regions meet.

The time-lapse photography method developed here was used to study the case of β to α transformation, but with only small changes could be used for studying the reverse transformation. Other future research fields where this method could be applied include the effect of temperature variations on the transformation rate and the study of the transformation in alloys, in particular lead-free alloys, which are of interest to the electronics industry.

6 CONCLUSIONS

This research has looked at possible ways of monitoring the tin pest transformation. These methods are based on some important characteristics of this phenomenon:

- Volume changes: this has been captured using a strain gauge measurement method. This method was sensitive to the initial phases of the transformation, but due to the expansion limitations of the strain gauges used, it could not be used after this point.
- Surface texture changes: from shiny metal to opaque grey: Furthermore many cracks form on the transformed material. These features were captured using a time-lapse photography method, that has proved very useful in explaining the mechanics of the transformation. The images and videos created with this method have highlighted how the stresses associated with the phase change tend to peel progressively away the surface of the material.
-
- Conductivity changes: This property formed the basis of the third monitoring method developed in this study, which consisted of a four-point electrical resistance measurement. In particular a full procedure of sample preparation and monitoring method was developed around this technique. Using this procedure an accelerated transformation could be obtained, and this was found to work also for tin alloys. Alloys would normally take too long to transform to be continuously monitored. Waiting 5 or 10 years to verify if an alloys is susceptible to the transformation is not a viable commercial option. Using an external seed as CdTe and InSb only partially solves the problem as for some alloys the incubation time can still be very long. The method developed here consists of hybrid alloys, where the seeds inoculates pure tin (which is a fast process) and then tin inoculates the alloy by gradually changing the composition. This accelerated transformation technique solves this problems and many different alloys could be ranked in terms of their transformation susceptibility. This method could be used as a standard technique for testing all the new lead-free tin bas alloys that are or will be commercialised. Although this study has shown the possibility for tin alloys to transform, it is still unknown if this could actually occur on a printed circuit board, where the presence of different surface finishes could change the nominal composition of the alloy. Also the small material amount in modern solder joints could influence the transformation, as the surface/volume ratio increases. Further research is then necessary to establish more clearly the risk involved in using lead-free alloys in low temperature environments, where the transformation is a possibility.

The results of the conductivity method also demonstrate that the transformation is possible in tin alloys with compositions that are typical of those of commercial alloys.

7 ACKNOWLEDGMENTS

We would like to thank the Department for Innovation, Universities and Skills (DIUS) for funding this research and Milos Dusek for his help in setting up some of the experiments and the software.

8 BIBLIOGRAPHY

- [1] J. H. Becker. On the quality of gray tin crystals and their rate of growth. *Journal of Applied Physics*, 29(1):1110–1121, 1956.
- [2] W. J. Plumbridge. Tin pest issues in lead-free electronic solders. *J Mater Sci:Mater Electron (2007)*, 18(1-3):307–318, 2007.
- [3] Plumbridge. Recent observations on tin pest formation in solder alloys. *Journal of Electronic Materials*, 37(2):218, 2008.
- [4] T. Nishimura K. Sweatman, S. Suenaga. Suppression of tin pest in lead free solders. In *Proceedings of JEDEX*, 2005.
- [5] W. Lee Williams. Gray tin formation in soldered joints stored at low temperature. Atlantic City, NJ, June 19-20 1956
- [6] E. O. Hall. The $\beta \rightarrow \alpha$ transformation in pure tin and its dilute alloys. Institute of Metals Monograph and Report Series, 1955.
- [7] A. D. Styrkas. Mechanism of the allotropic transformation of sn. *Inorganic Materials*, 39(8):806–810, 2003.
- [8] R. M. Organ H. J. Plenderleith. The decay and conservation of museum objects of tin. *Studies in Conservation*, 1(2):63–72, 1953.
- [9] A. D. Styrkas. Sn infection in liquid h₂o. *Inorganic Materials*, 39(8):940–943, 2003.
- [10] A. D. Styrkas. Growth of gray tin crystals. *Inorganic Materials*, 39(7):808–811, 2003.
- [11] A. D. Styrkas. Preparation of shaped gray tin crystal. *Inorganic Materials*, 41(6):671–675, 2005.
- [12] J. Spergel. Tin transformation of tinned copper wire. *ASTM Special Tech. Pub.*, 319, 1962.
- [13] A. Hallbrucker Erwin Mayer. Cubic ice from liquid water. *Nature*, (325):601–602, 1987.
- [14] A. Bornemann. "tin disease" in solder type alloys. *ASTM Special Tech. Pub.*, 189, 1956.

- [15] G. J. Dienes J. Fleeman. Effect of reactor irradiation on the white-to-grey tin transformation. *Journal of Applied Physics (U.S.)*, 26:652–654, 1955.
- [16] W. R. Lewis. *Tin Solders at Low Temperatures*. Notes on Soldering. Tin Research Institute, 1968 reprint.
- [17] Herbert Ipser Olga Semenova, Hans Flandorfer. On the non-occurrence of tin pest in tin-silver-indium solders. *Scripta Materialia*, 52:89–92, 2005.
- [18] L. J. Groen W. G. Burgers. Mechanism and kinetics of the allotropic transformation of tin. *Discuss. Faraday Soc.*, 23:183 – 195, 1957.
- [19] G. V. Raynor R. W. Smith. The effect of liquid media on the grey tin-white tin transformation in commercially pure tin. *Proceedings- Physical Society Section B.*, 70(12):1135–1142, 1957.
- [20] R. Rogers; J. F. Fydell. Effect of germanium on the transformation of white to gray tin, at comparatively low temperature. *Journal Electrochemical Society*, 100(4):161–164, 1953.
- [21] F. Vnuk. Preparation of compact α -tin specimens. *Journal of Crystal Growth*, 48(3):486–488, 1980.